The New Weather Station for the VLA

Bryan Butler, Wayne Koski
EVLA Memo 179
May 13, 2014

1.0 Introduction

The weather station of the VLA (see e.g. Clark 1987) was replaced as part of the EVLA upgrade. This memo describes the location of the new weather station, its tower and instrumentation, some comparisons with the old VLA weather station and the LWA weather station, and some notes about access to displays of the information from it. Note that the tower and instrument measurement accuracy requirements are given in Butler & Perley (2008).

2.0 Location and Instrument Tower

The weather station instruments are mounted on a tower located east of the Cafeteria (just northeast of where the easternmost VSQ building used to be, next to the RFI tower - see Figure 1). The tower is a Rohn 45G, 60' fixed guyed tower, with instruments at or near the top and a junction box at the bottom. Having the instruments at that height puts them near where the vertex room of the antennas is, which is desirable. Figure 2 shows the geometry of the tower and the instruments. Figure 3 shows a closeup of the recommended layout of instruments on the boom, which we have mostly followed. Figure 4 shows actual photographs of the installed tower (without the instruments), and Figure 5 shows the top of the tower with the horizontal boom and the sensors, shields, and transmitters installed.

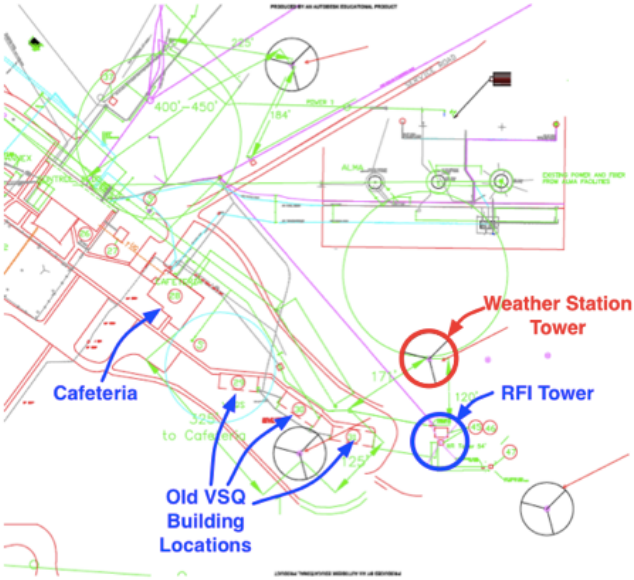

Figure 1. The location of the new weather station tower at the VLA site.

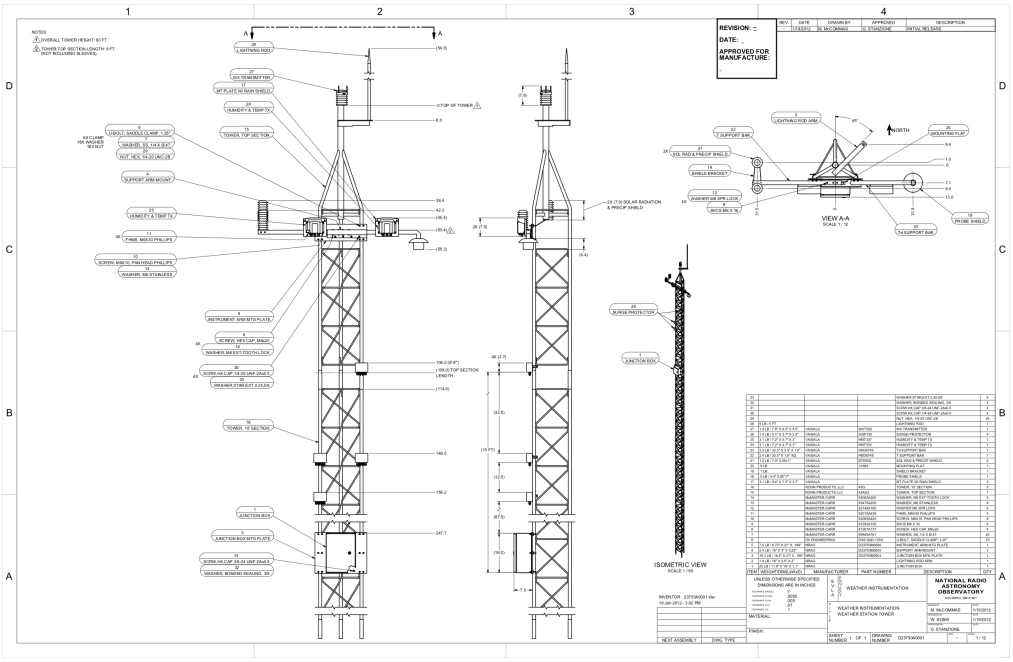

Figure 2. The geometry of the Rohn 45G 60' tower, along with the instrument boom, junction box, and protective lightning rod.

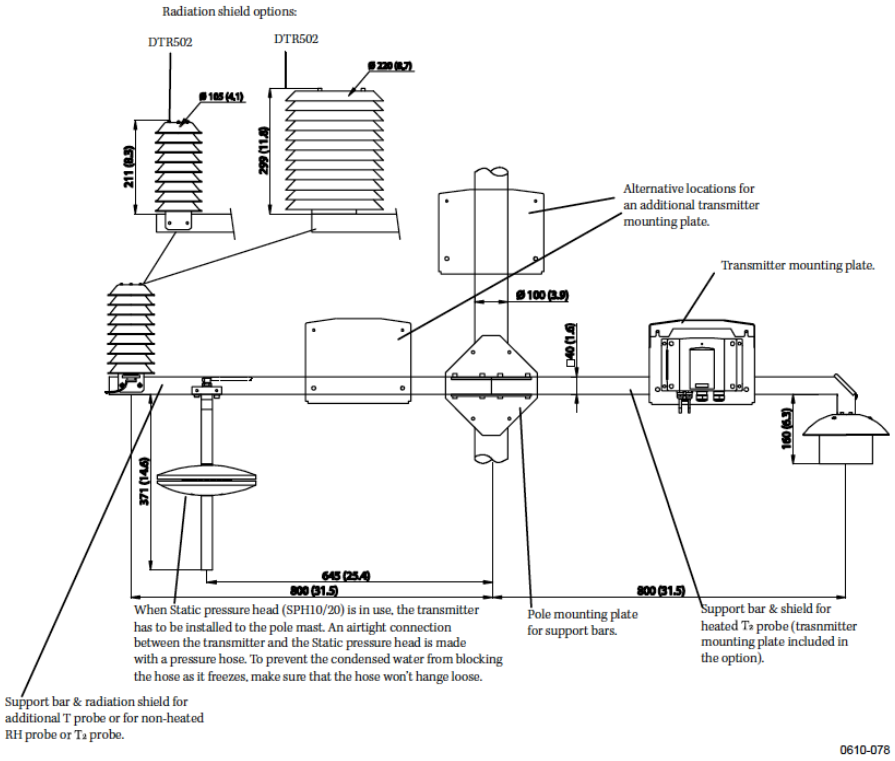

Figure 3. Recommended layout of instruments on instrument boom, from Vaisala documentation. We have mostly followed these recommendations (see Figure 5).

Figure 4. The weather tower, without instrumentation, at the VLA site. On the left is the entire 60' tower (with ALMA ATF antennas and a VLA antenna in the background); on the right is just the top of the tower.

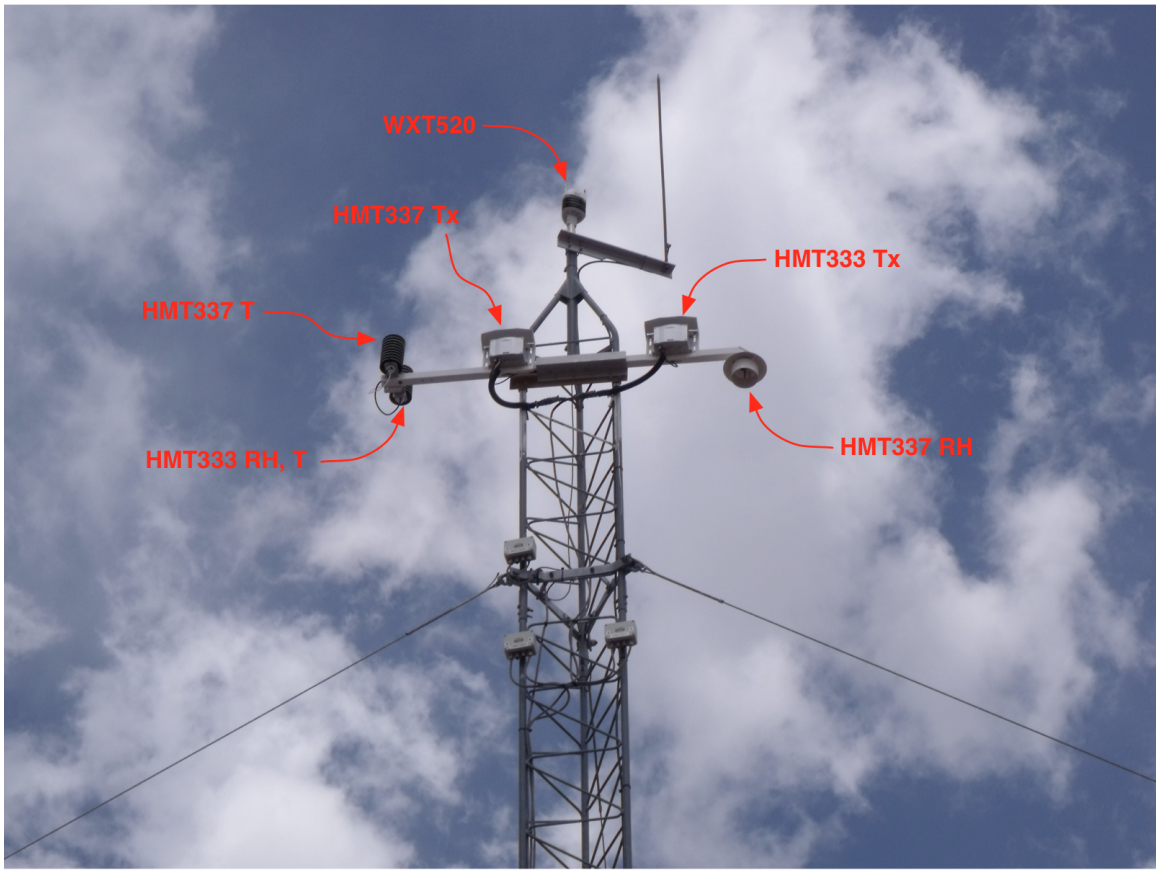

Figure 5. The top of the tower at the VLA site with the instrumentation installed. Abbreviations: Tx=transmitter; T=temperature sensor; RH=relative humidity sensor. Picture courtesy Jerry Langevin.

3.0 Instruments

We have to measure five fundamental quantities at the site: temperature, relative humidity (or dew point temperature), pressure, wind speed, and wind direction. Temperature, relative humidity, and pressure are used in the calculation of the total delay and the antenna pointing offset from refraction during observing. Wind speed is used in scheduling observations. Wind direction is only informational right now but might also be used eventually in scheduling. We have three separate instruments to measure these five quantities, some of which provide redundant measurements. We measure temperature and relative humidity with a Vaisala HMT337 and HMT333. The only difference between them is that the HMT337 has a heated probe (see discussion below). We measure pressure, wind speed, and wind direction with a Vaisala WXT520. The WXT520 also measures precipitation, and temperature and relative humidity, but the temperature and relative humidity are measured with less accuracy than the HMT337 and HMT333 (see the following sections for details on accuracy).

In addition to these fundamental measurements, we provide two additional instruments to measure information that may be of use to astronomers in understanding the atmospheric conditions during their observations: two LI-COR LI-200 pyranometers to measure solar irradiance, and an all-sky camera (Arecont AV20365DN 360^{o} panoramic camera) to potentially measure cloud cover.

3.1 HMT337

The Vaisala HMT33x series of instruments measure relative humidity with a HUMICAP 180 sensor. This is a thin film polymer capacitive sensor. While not as accurate as a chilled mirror hygrometer, it is much easier to maintain and less sensitive to things like mirror contamination, and meets our basic relative humidity measurement requirement. Figure 6 shows the HMT337 probe and transmitter. This unit also has a heated probe (the heater is the thin black rod attached to the transmitter by the white wire in Figure 6). The advantage to having the heater is that if the HUMICAP sensor gets wet (from direct rain or dew/frost condensation on the probe), readings are affected for many hours (see Figure 7). We do have a rain/radiation shield over the probe, but that will not prevent dew/frost. In any event, the heater prevents this from occurring.

The accuracy of the relative humidity measurement is ±1% from 0-90% RH and ±1.7% from 90-100% RH at +15 to +25 ^{o}C, ±(1+RH/125)% at -20 to +40 ^{o}C , and ±(1.5+RH/67)% at -40 to +180 ^{o}C. For all practical conditions at the VLA site this means better than 1.5% accuracy. There is an additional calibration uncertainty of 1%. The response time (to 90%) of the unit with our filter (grid + steel netting) is 20s. The unit also has an ambient temperature sensor – a "Pt100 RTD 1/3 Class B IUEC 751" – i.e., a platinum resistance thermistor. The accuracy of this measurement is in the range of 0.2 to 0.3 ^{o}C given typical ambient temperatures at the site. The details of the accuracy of the measurement as a function of the ambient temperature are shown in Figure 8.

The HMT337 unit itself calculates and provides a number of other meteorological quantities from the fundamental measurements of temperature and

relative humidity: dewpoint temperature, water vapor mixing ratio, absolute humidity, wet bulb temperature, enthalpy, and water vapor pressure.

Figure 6. The Vaisala HMT337 relative humidity probe and transmitter. The heater is the black rod attached to the transmitter by the white wire. Note that the HMT333 unit is a duplicate of this, but without the heated probe.

3.2 HMT333

The HMT333 unit is a duplicate of the HMT337 unit, but without the heated probe. Under most conditions it should perform exactly the same. As mentioned above, the only exception to this is when there is moisture on the sensor (most importantly, when there is frost or dew that forms).

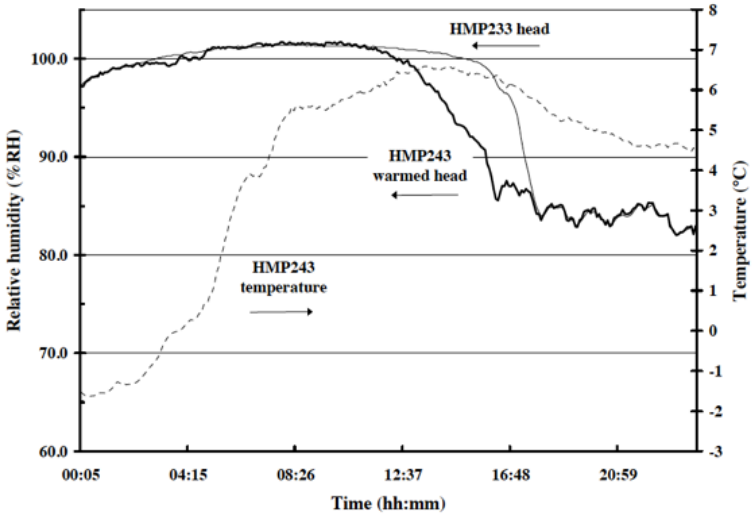

Figure 7. A demonstration of the problem with dew/frost formation on a non-headed RH probe vs. one that is heated. The HMP233 is the equivalent of our HMT333 probe (not heated), while the HMT243 is the equivalent of our HMT337 probe (heated). After dew/frost forms on the probes, there is a several-hour lag before the non-heated probe measures the proper value. From Ranta-aho & Stormbom (2002).

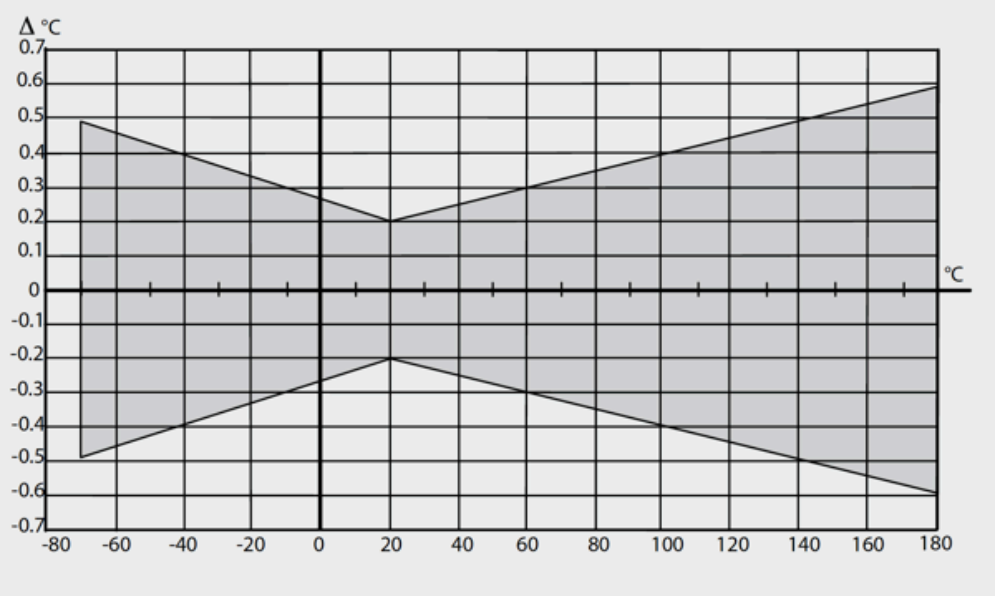

Figure 8. The temperature measurement accuracy of the HMT33x devices, as a function of ambient temperature. For the VLA, under most conditions, the accuracy should be from 0.2 to 0.3 °C.

3.3 WXT520

The Vaisala WXT520 weather instrument measures six weather parameters, from a small (~20 cm tall and ~12 cm wide) and lightweight (0.65 kg) package. It measures wind speed and direction, precipitation, atmospheric pressure, temperature, and relative humidity. Figure 9 shows a picture and cutaway diagram of the instrument and its various sensors.

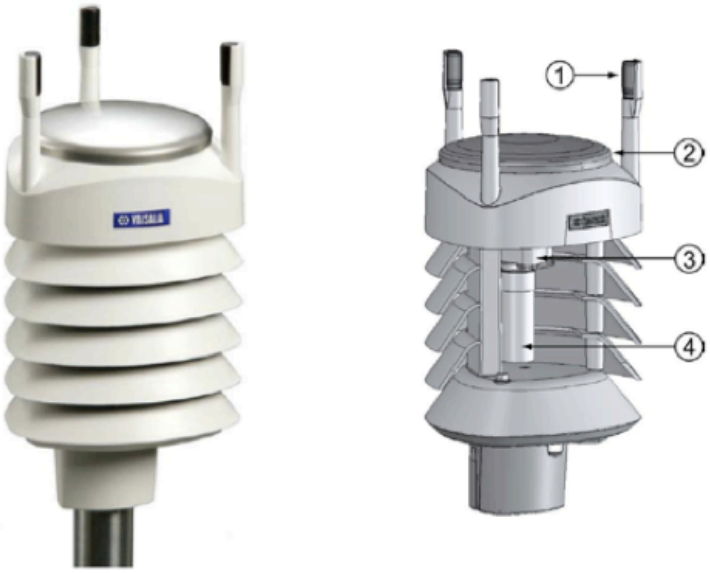

Figure 9. The Vaisala WXT520 weather transmitter. On the left is a picture, on the right a cut-away diagram. In the cut-away, item 1 is one of three wind transducers; 2 is the precipitation sensor; 3 is the pressure sensor; and 4 is the humidity and temperature sensors.

3.3.1 WXT520 Wind Measurement

Wind is measured with a WINDCAP sensor that uses ultrasound to determine horizontal wind speed and direction. It does this with an array of three equally spaced transducers, as can be seen in Figure 9. The wind speed measurement range is 0 to 60 m/s. On occasion, winds get stronger than this at the site, and we may not be able to measure these very strong winds. The accuracy at speeds from 0 to 35 m/s is ±0.3 m/s or ±3%, whichever is greater. From 35 to 60 m/s the accuracy is ±5%. The output precision is 0.1 m/s. The accuracy and precision of the wind direction measurement is ±3^{o} and 1^{o}, respectively. The response time of the device is 250 ms. Note that since the WXT520 measures wind direction, it needs to be mounted in a particular geometry. To do this, there is an arrow and the text "North" on the bottom of the transmitter, which needs to be aligned to true North. Since the tower is fixed (cannot be lowered), this must be done at the top of the tower (and is currently done with a hand-held compass), which can be difficult depending on current conditions (how windy it is, notably). We have discussed better ways to set this direction, but nothing has been done about it yet. If it is clear that there is an offset, the software in the device can be set to account for that offset. See the discussion in the wind direction data section below.

3.3.2 WXT520 Precipitation Measurement

Precipitation is measured with a RAINCAP sensor that is a steel cover over a piezoelectric detector. The device detects the impact of individual rain or hail drops and converts them into intensity and accumulated precipitation. It can distinguish between rain and hail, as well as filtering out other non-rain and non-hail impacts. Rain intensity is measured over one-minute running averages, with a range of 0 to 200 mm/h (broader with reduced accuracy), an accuracy of ±5% (though spatial variations in rainfall make this hard to estimate), and an output precision of 0.1 mm/h. Rain accumulation is estimated to have a similar accuracy, with a precision of 0.01 mm. Hail intensity has no specified accuracy, and a precision of 0.1 hits/cm^{2}h. Hail accumulation has a precision of 0.1 hits/cm^2.

3.3.3 WXT520 Pressure Measurement

Pressure is measured with a capacitive silicon BAROCAP sensor, contained along with the temperature and relative humidity sensors in the PTU module. It has a measurement range of 600 to 1100 hPa. The accuracy is ±0.5 hPa from 0 to 30^{o} C, and ±1 hPa outside that range. The output precision is 0.1 hPa. The response time of the device is 500 ms.

3.3.4 WXT520 Temperature Measurement

Temperature is measured with a capacitive ceramic THERMOCAP sensor, contained along with the pressure and relative humidity sensors in the PTU module. It has a measurement range of -52 to +60 ^{o}C . The accuracy is a function of the

ambient temperature, and is shown in Figure 10. For typical VLA temperatures it is in the range 0.2 to 0.4 °C. The output precision is 0.1 °C. The response time of the device is unknown.

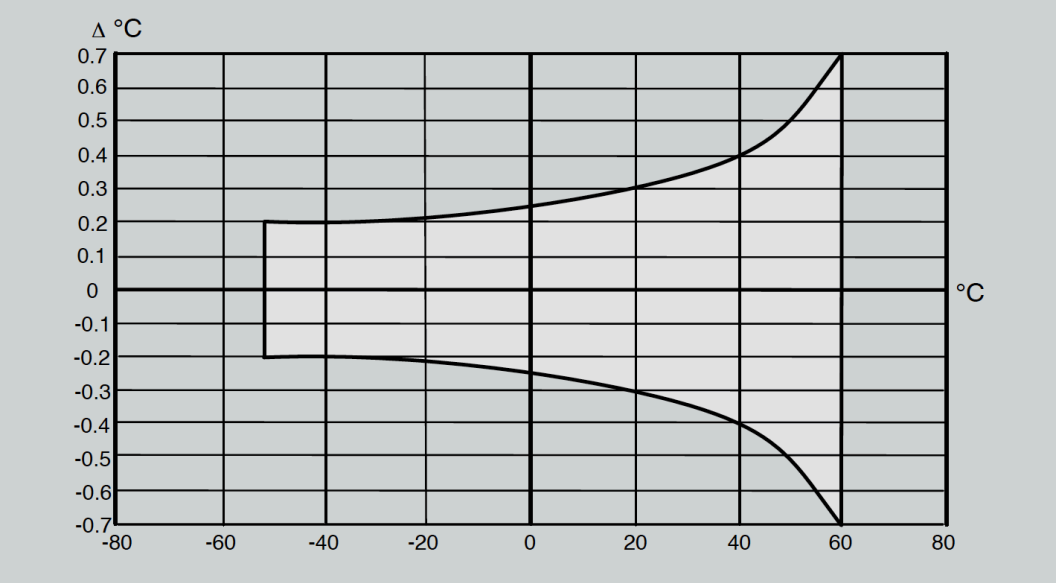

Figure 10. The temperature measurement accuracy of the WXT520 device, as a function of ambient temperature. For the VLA, under most conditions, the accuracy should be from 0.2 to 0.4 °C.

3.3.5 WXT520 Relative Humidity Measurement

Relative humidity is measured with a capacitive thin film polymer HUMICAP 180 sensor, contained along with the pressure and temperature sensors in the PTU module. It has a measurement range of 0 to 100% RH . The accuracy is ±3 %RH from 0 to 90 %RH, and ±5 %RH from 90 to 100 %RH. The output precision is 0.1 %RH. The response time of the device is unknown.

3.4 Pyranometer

A pyranometer is a device for measuring broadband solar irradiance. There are two pyranometers, mounted on top of the junction box at the bottom of the weather station tower – one looking vertically; one looking south at roughly the VLA site latitude from vertical. These are Li-Cor LI200 sensors; Figure 11 shows one of them, while Figure 12 shows them as installed at the VLA site. Figure 13 shows the spectral response of the devices. We are not currently using these devices for any scheduling or other operational purposes, but may do so in the future

Figure 11. The Li-Cor LI200 pyranometer, for measuring broadband solar irradiance.

Figure 12. The pyranometers as installed at the VLA site. Pictures courtesy Jerry Langevin.

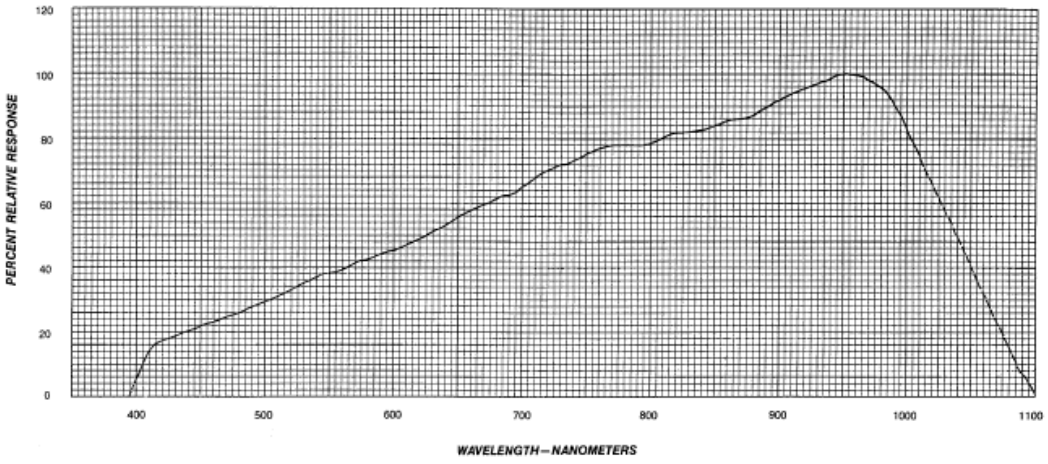

Figure 13. The spectral response of the pyranometers.

3.5 All-sky Camera

There is an all-sky camera that is yet to be mounted on top of the junction box below the weather station tower. It was intended that this would mostly be for qualitative information about conditions during observing, but more quantitative uses may be discovered (for instance, the actual camera we purchased has some response into the infrared, so might serve to measure cloud cover, but this remains to be tested). This is an Arecont AV20365DN camera, as shown in Figure 14. The camera is roughly 18 cm tall and 18 cm in diameter. It has four lenses, which allow it to take a full 360^{o} panoramic picture. Each lens is backed by a 5 Megapixel CMOS CCD, for 20 Megapixels total on every full picture. It is capable of sending these images out at 3.5 images per second, but our intent is to only capture these and archive them at several minute intervals. Before it can be installed at the site, it must be fully RFI-tested, and put into an RFI (and weather) enclosure.

Figure 14. The all-sky camera. Four wide-angle lenses allow full hemispheric coverage above the site.

3.6 Instrument Calibration

We had two options for calibration of the three main (Vaisala) weather station instruments: either purchase a calibration unit and perform the calibration ourselves, or send the instruments to Vaisala for calibration there. Since we have no experience calibrating these devices, and since the calibration unit, the HMK15 (and its calibration salts) are rather expensive, we opted to send the units to Vaisala for calibration. One additional advantage of having the units calibrated at Vaisala is that it provides NIST traceability. We have two of each of the units, and the calibrations are good for one year. So we exchange each set of instruments every six months, sending the unit that has been deployed at the site out for calibration.

4.0 Data

During the month of May 2012, we ran the new weather station while keeping the old weather station operational. Unfortunately, the old weather station chilled mirror hygrometer was broken at this time so we have no comparison of the humidity measurements. We can compare the new instruments against each other, however, and we can also compare them with measurements from the LWA weather station. The LWA weather station is a less precise one (a Davis Vantage Pro 2), but provides an additional comparison nonetheless.

For each of the measured quantities, we will show a plot of the measurement for the full month, for one week, and for one day. Then we will show histograms of the differences between measurements with the HMT333, HMT337, WXT520, old VLA weather station (hereafter referred to as DCS00), and the LWA weather station.

4.1 Temperature

Figures 15, 16, and 17 show temperature measurements for the HMT337 in May 2012. The known diurnal variations are clearly seen, though since the measurement is made at ~60' height, they are slightly different than the normal expected surface temperature diurnal variations. There is a curious phenomenon seen in daytime – there is a clear fluctuation in the temperature which is much larger than the noise of the instrument. We surmise that this is due to convective instability in the surface layer at the VLA site. As the ground heats up in the morning, it causes the surface layer to become unstable, which causes turbulent fluctuations. Since the measurement is made at 60', it is these fluctuations we see in the plots. The fluctuations seem to be of the order of a few tenths of a degree C.

Figures 18-21 show differences between the measurement of the HMT337 (which we take as the most accurate of the measurements) and the HMT333, the DCS00, and the LWA. It is clear that the HMT337 and HMT333 agree quite well. Agreement with the WXT520 is also good, but there is a clear bias of a few tenths of a degree C. Agreement with the DCS00 is not as good – the distribution is much wider (several degrees C) and there seem to be two Gaussian distributions, one centered around 0.5 ^{o}C and one centered around -1.5 ^{o}C. Agreement with the LWA is similar to DCS00. Table 1 shows the median offset of the distributions, as well as the standard deviation, if a single Gaussian is assumed (clearly not true for the DCS00 and LWA differences). We estimate the standard deviation by calculating the Median Absolute Deviation (MAD) and multiplying by 1.4826. This is a robust statistic, and since we have outliers in the differences is appropriate (Hampel 1974).

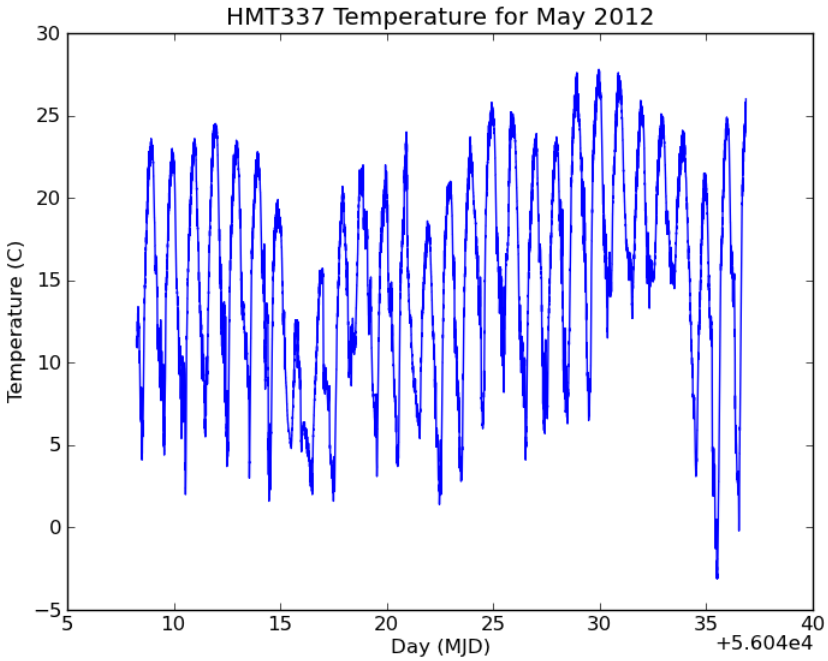

Figure 15. Measured temperature for the month of May 2012 with the HMT337 instrument. Diurnal variations are apparent, as are longer-term (of order one week) variations.

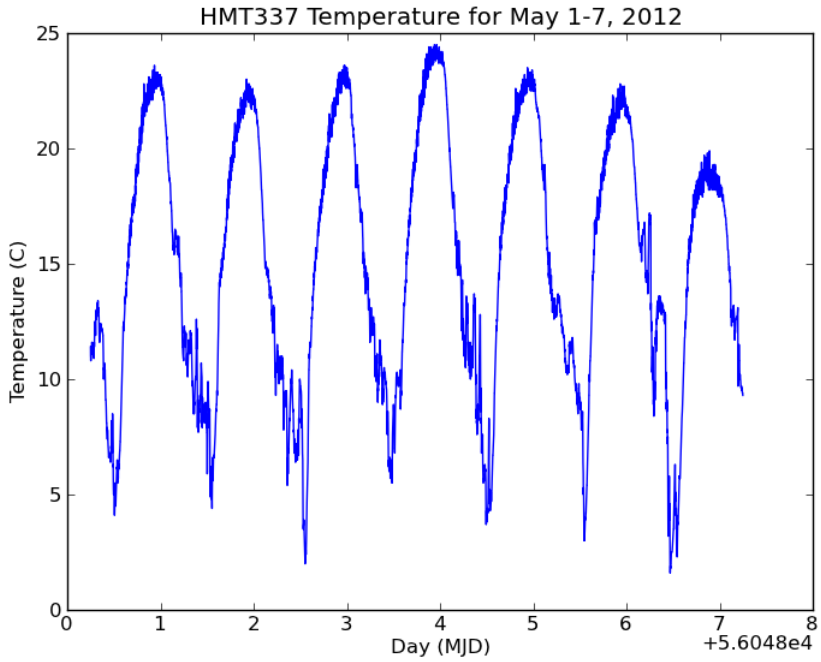

Figure 16. Measured temperature for the week of May 1-7, 2012 with the HMT337 instrument. Diurnal variations are apparent, as are some shorter term variations.

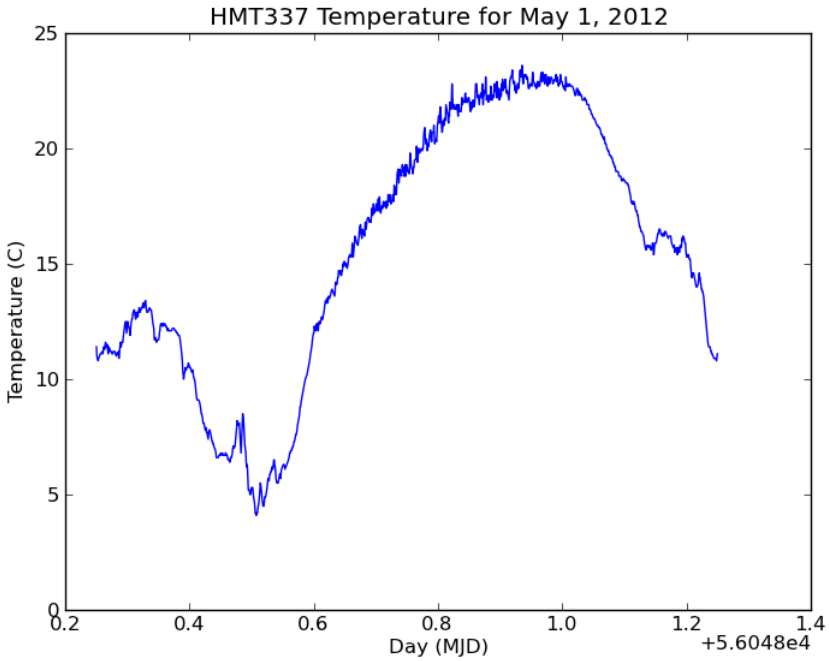

Figure 17. Measured temperature for May 1, 2012 with the HMT337 instrument. The diurnal variation is apparent, as is an increase in noise during daytime.

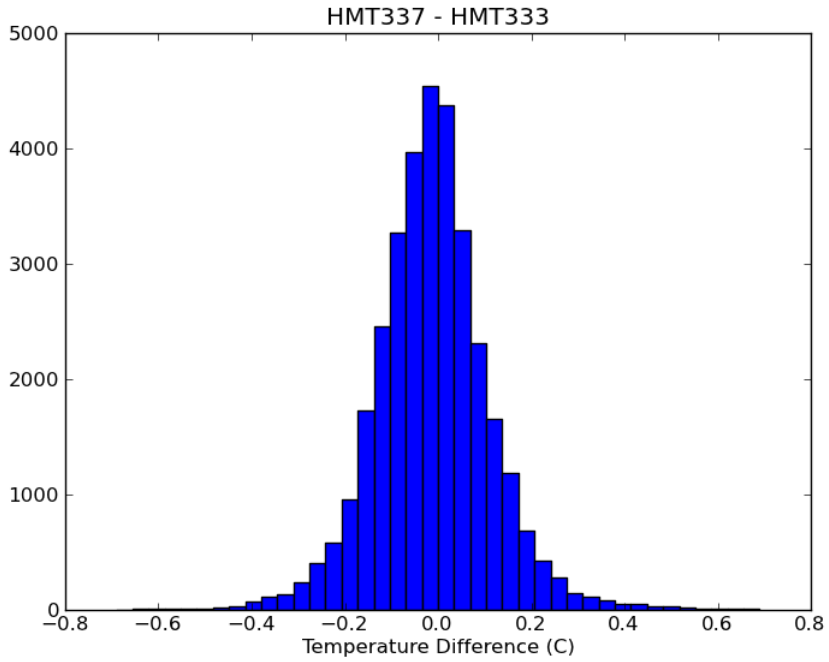

Figure 18. Histogram of the difference between the temperature measurements of the HMT337 and HMT333 for May 2012.

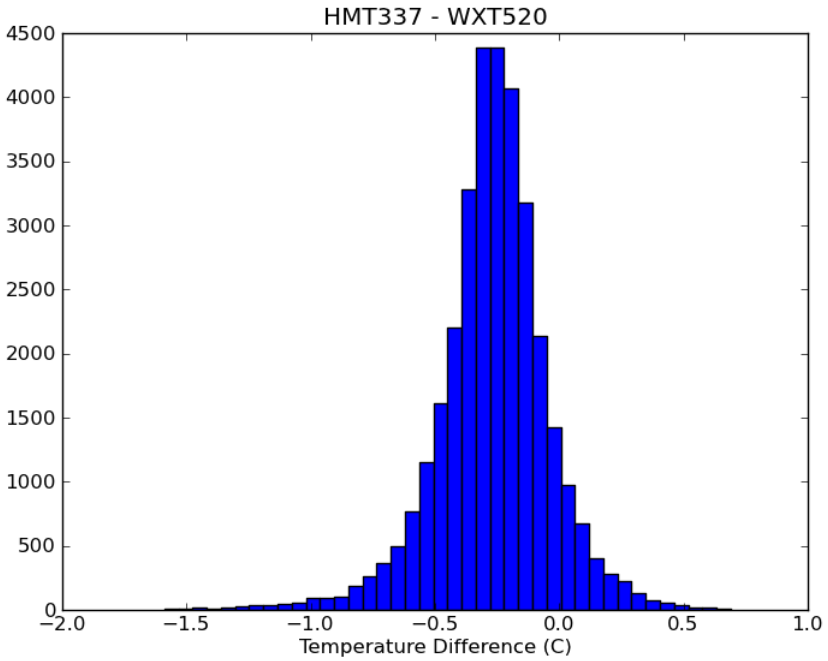

Figure 19. Histogram of the difference between the temperature measurements of the HMT337 and WXT520 for May 2012.

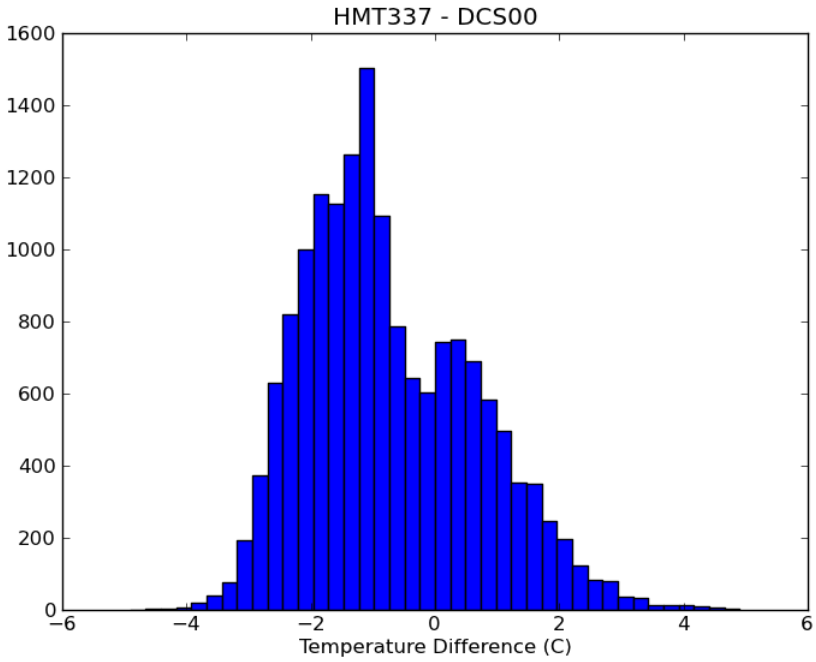

Figure 20. Histogram of the difference between the temperature measurements of the HMT337 and the old VLA weather station (DCS00) for May 2012.

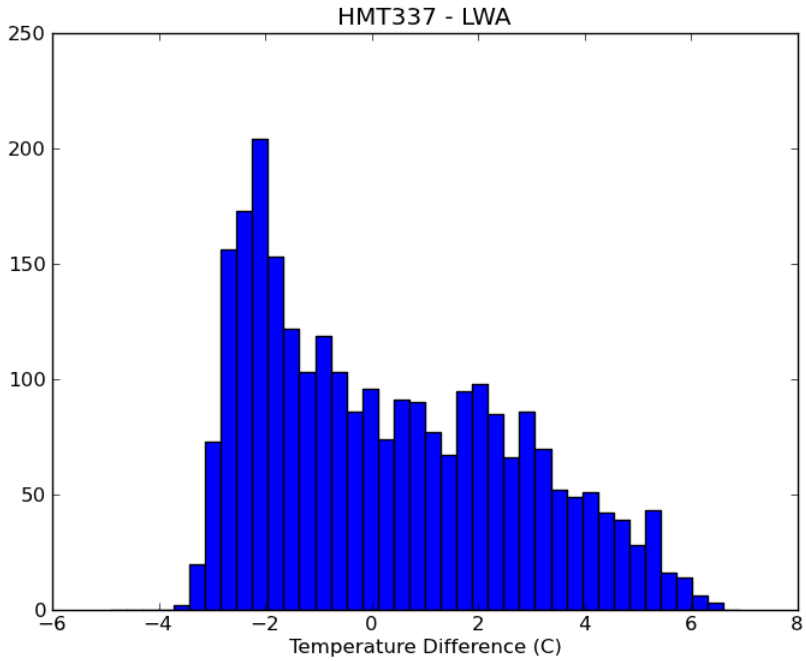

Figure 21. Histogram of the difference between the temperature measurements of the HMT337 and the LWA weather station for May 2012.

Table 1. Median and standard deviation of differences in temperature measurements for May 2012.

Quantity	Median (°C)	Std Dev (MAD * 1.4826) (°C)
HMT337 – HMT333	-0.01	0.11
HMT337 – WXT520	-0.26	0.18
HMT337 – DCS00	-1.00	1.43
HMT337 – LWA	-0.13	2.87

4.2 Relative Humidity

Figures 22, 23, and 24 show relative humidity measurements for the HMT337 in May 2012. The known diurnal variations are clearly seen, with higher relative humidity at night (due to lower temperatures). There is a similar phenomenon seen in daytime as with temperature (increased fluctuations), which we attribute to the same cause.

Figures 25-28 show differences between the measurement of the HMT337 (which we take as the most accurate of the measurements) and the HMT333, the DCS00, and the LWA. The HMT337 and HMT333 agree fairly well, but there is a clear bias, and there is also a long tail on both sides of the histogram. Agreement with the WXT520 is also good, but there is a similar bias and long tail. In addition, there is an odd stair-stepping phenomenon in the histogram, which we do not understand. Given that the bias in both the HMT337-HMT333 and HMT337-

WXT520 histograms is in the same direction and roughly equal magnitude, this may indicate a true offset in the HMT337, but we assume this has been fixed by the most recent calibration of the sensors at Vaisala. Because of the odd stair-stepping in the histogram, we have also plotted the histogram of the difference between the HMT333 and the WXT520 in Figure 27. That histogram does not demonstrate that phenomenon. Again, we do not understand its origin. The agreement with the LWA measurement is poor – with a central core distribution and a much broader second one. Table 2 shows the median offset of the distributions, as well as the standard deviation, if a single Gaussian is assumed.

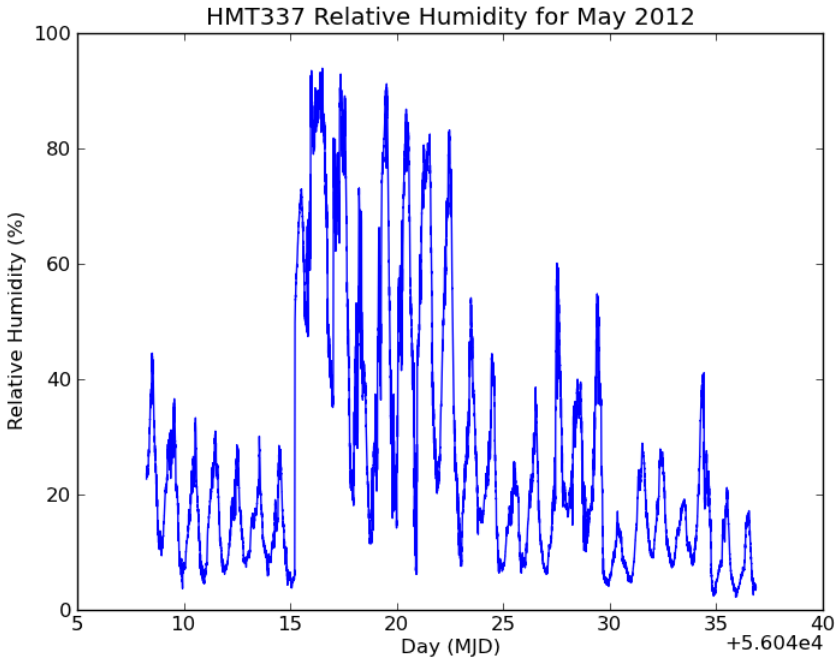

Figure 22. Measured relative humidity for the month of May 2012 with the HMT337 instrument. Diurnal variations are apparent as are longer-term (of order one week) variations.

Table 2. Median and standard deviation of differences in relative humidity measurements for May 2012.

Quantity	Median (%)	Std Dev (MAD * 1.4826) (%)
HMT337 – HMT333	-0.8	0.30
HMT337 – WXT520	-0.9	0.45
HMT333 – WXT520	-0.1	0.59
HMT337 – LWA	-5.2	2.08

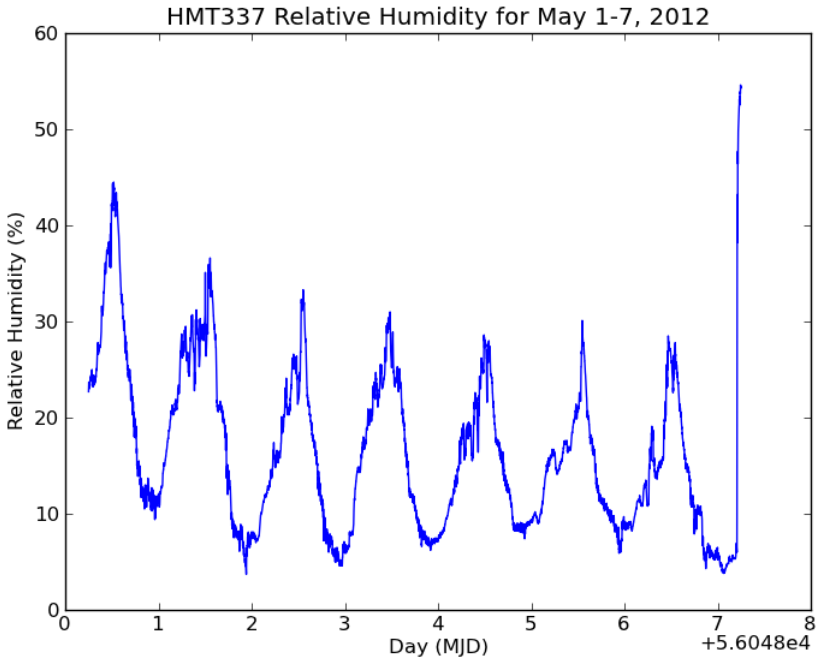

Figure 23. Measured relative humidity for the week of May 1-7, 2012, with the HMT337 instrument. Diurnal variations are apparent, with higher relative humidity in nighttime.

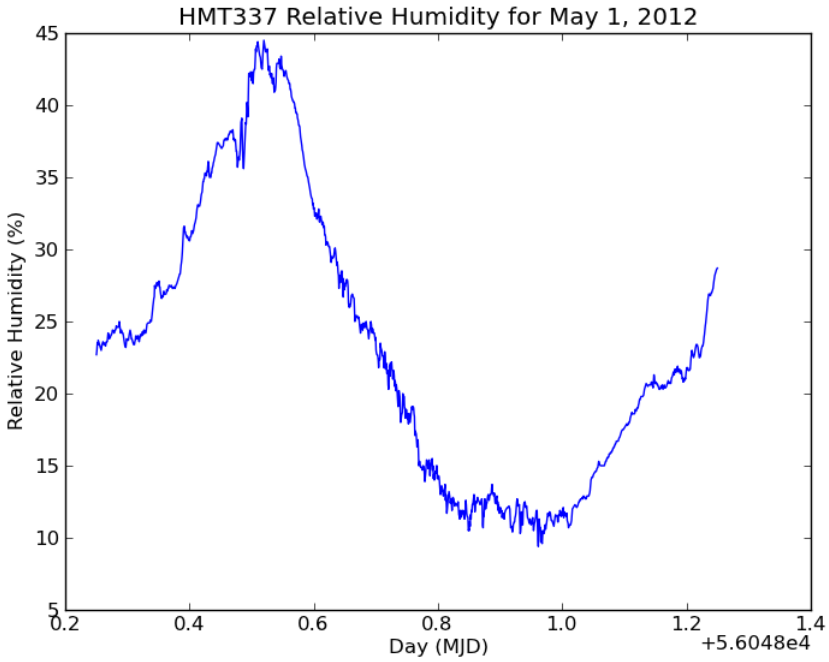

Figure 24. Measured relative humidity for May 1, 2012 with the HMT337 instrument. The diurnal variation is apparent, with relative humidity higher in nighttime.

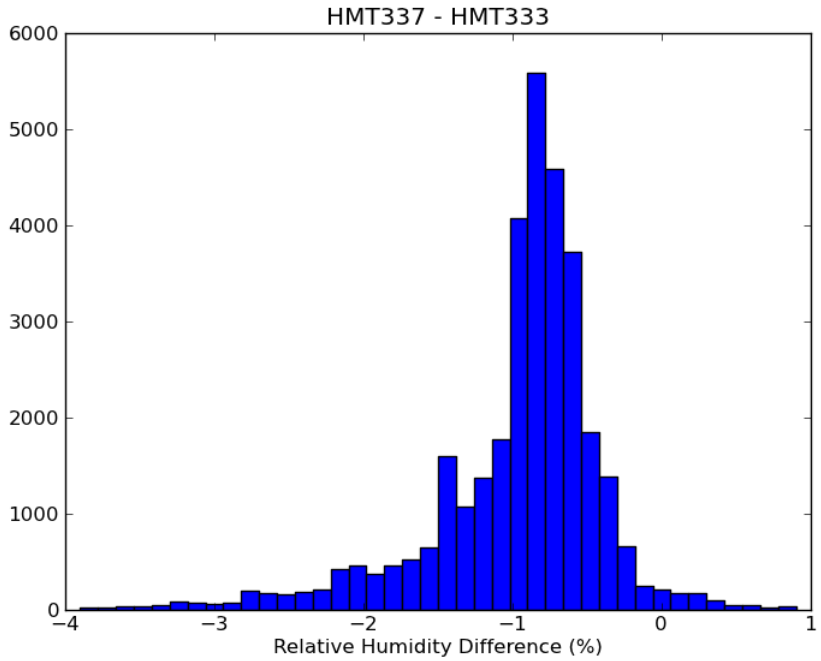

Figure 25. Histogram of difference between the relative humidity measurements of the HMT337 and HMT333 for May 2012.

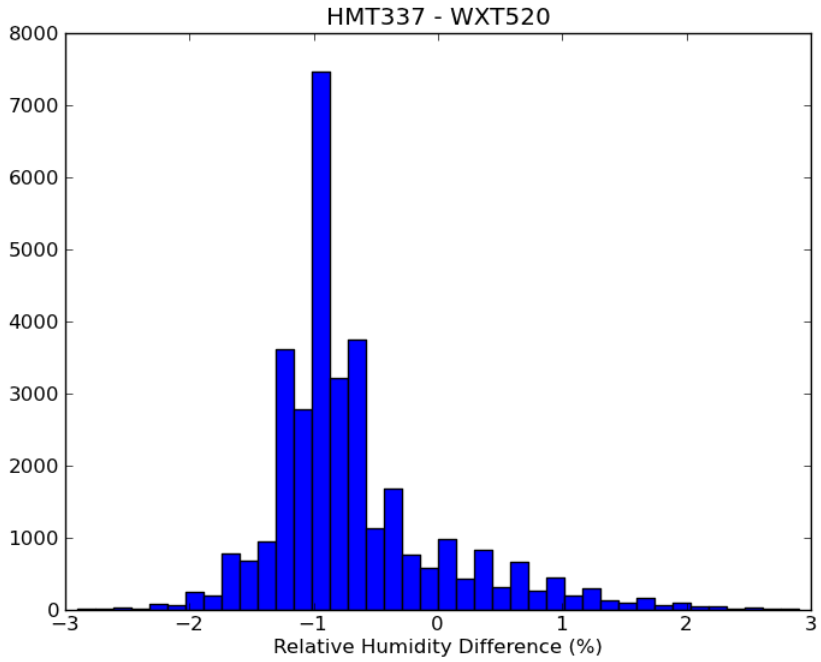

Figure 26. Histogram of the difference between the relative humidity measurement of the HMT337 and the WXT520 for May 2012. There is an odd stair-stepping in the histogram which we do not understand.

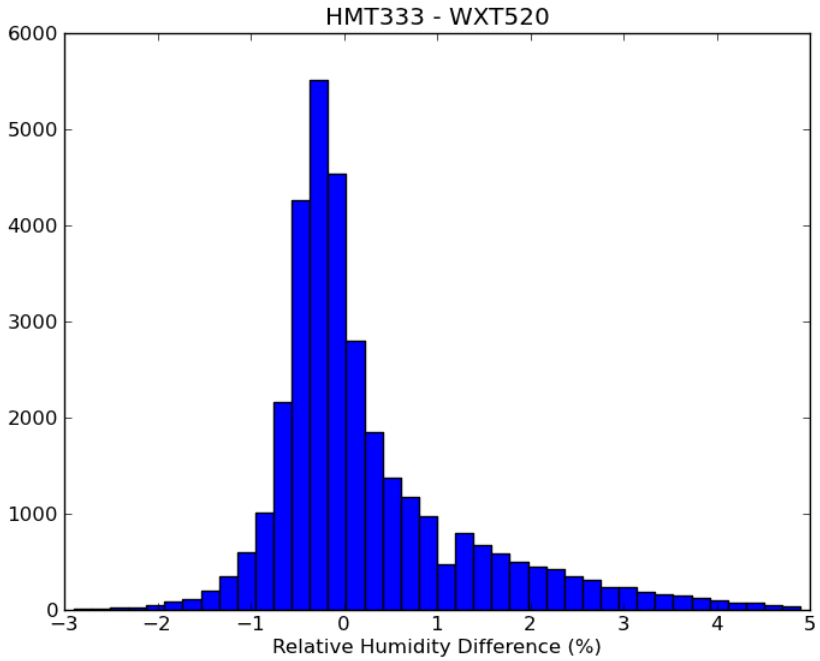

Figure 27. Histogram of the difference between the relative humidity measurement of the HMT333 and WXT520. The stair-stepping in Figure 26 is not apparent here.

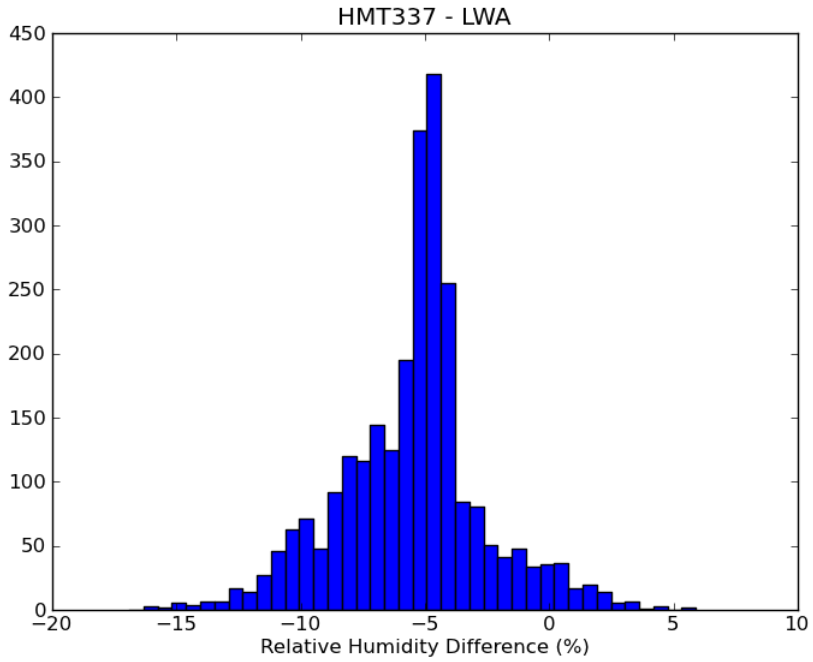

Figure 28. Histogram of the difference between the relative humidity measurement of the HMT337 and the LWA. There is a core Gaussian distribution with width of a few %, and a much broader one with a width of ~10%.

4.3 Wind Speed

Figures 29, 30, and 31 show wind speed measurements for the WXT520 in May 2012. The known diurnal variations are clearly seen, with higher wind speeds during daytime. There is a similar phenomenon seen in daytime as with temperature (increased fluctuations), which we attribute to the same cause.

Figures 32 and 33 show differences between the measurement of the WXT520 (which we take as the most accurate of the measurements) and the DCS00 and LWA. The difference between the old VLA weather station and the WXT520 seems to be composed of two Gaussians – one centered at about 0.5 m/s with width of about 1 m/s, the other with a much larger offset (2 m/s) and width (5 m/s). The old VLA weather station wind sensor was known to be misbehaving at this point in time, which is probably the cause of the disagreement. The difference between the WXT520 and the LWA seems similar to the wider one in Figure 32 – an offset of about 2 m/s with a width of about 5 m/s. The fact that the offsets for the old VLA and LWA weather stations are both positive and of the same order is a slight concern – we would like to get another independent measure of this to verify that the WXT520 is actually reading the proper wind speed. Table 3 shows the median offset of the distributions, as well as the standard deviation, if a single Gaussian is assumed.

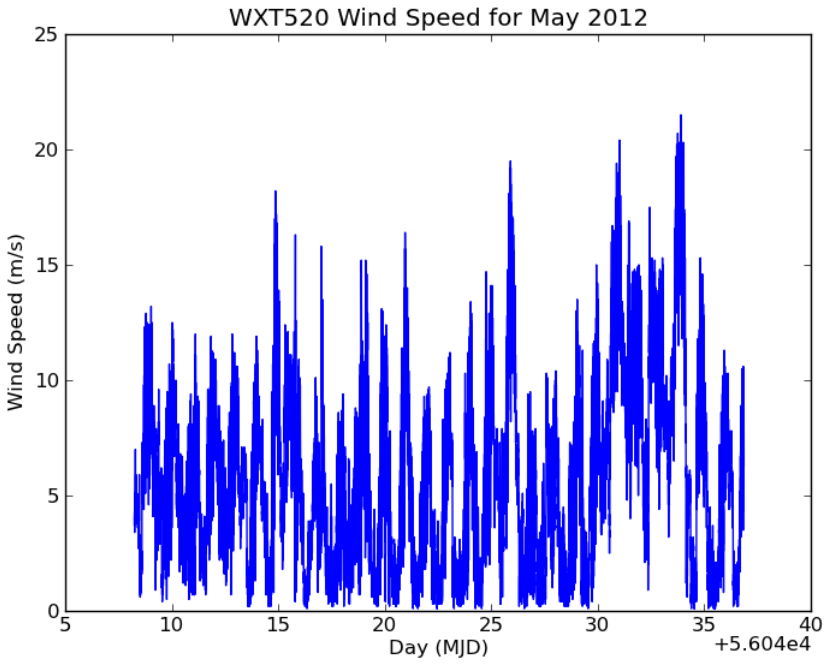

Figure 29. Measured wind speed for the month of May 2012 with the WXT520 instrument. Diurnal variations are apparent as are longer-term (of order one week) variations.

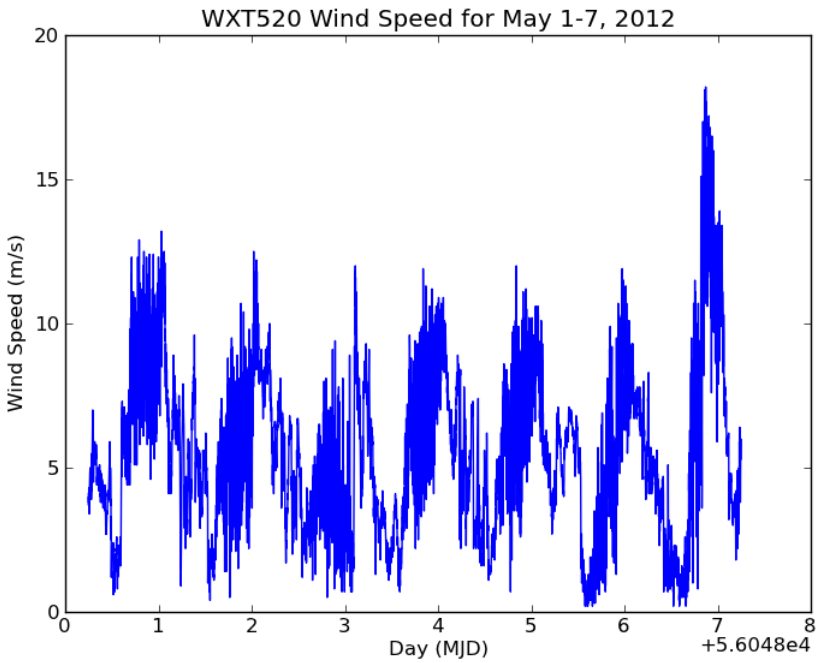

Figure 30. Measured wind speed for the week of May 1-7, 2012, with the WXT520 instrument. Diurnal variations are apparent, as is the fact that the wind speed fluctuates much more during daytime.

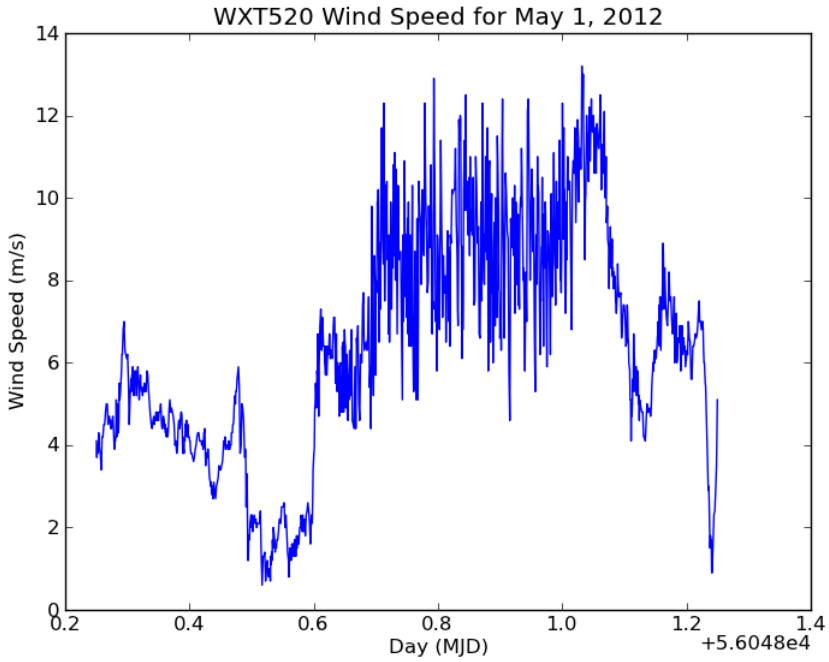

Figure 31. Measured wind speed for May 1, 2012, with the WXT520 instrument. Here the larger fluctuations during daytime are quite obvious.

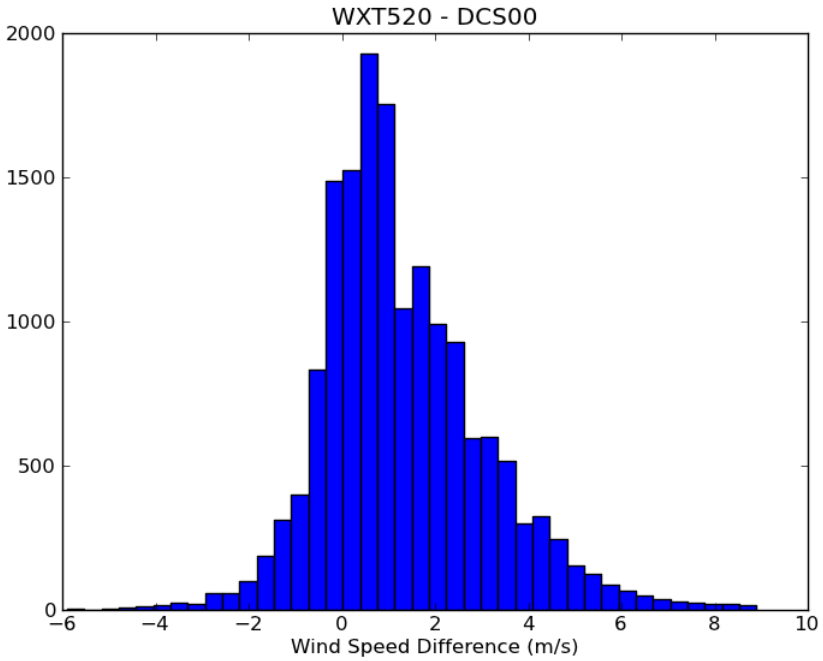

Figure 32. Histogram of the difference between the wind speed measurements of the WXT520 and the old VLA weather station for May 2012.

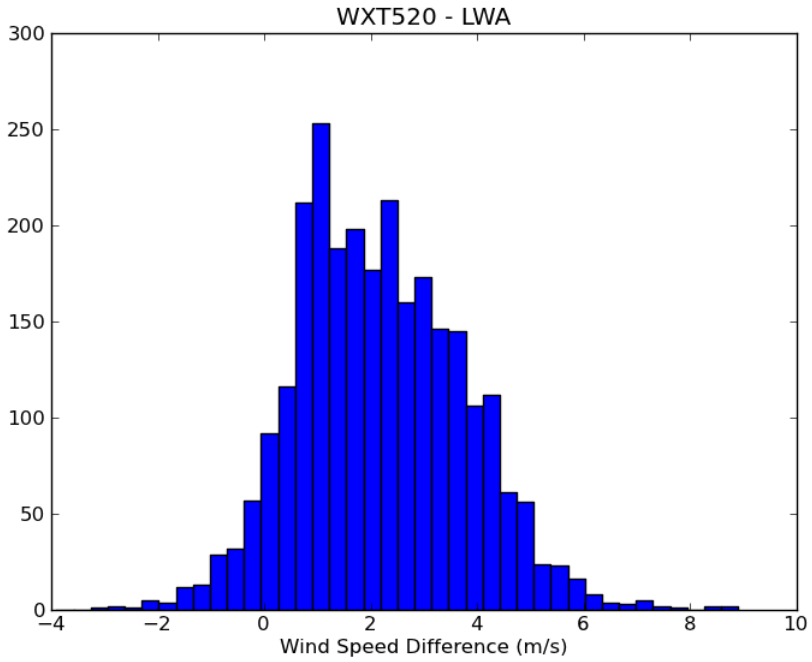

Figure 33. Histogram of the difference between the wind speed measurements of the WXT520 and the LWA weather station for May 2012.

Table 3. Median and standard deviation of differences in wind speed measurements for May 2012.

Quantity	Median (m/s)	Std Dev (MAD * 1.4826) (m/s)
WXT520 – DCS00	1.0	1.5
WXT520 – LWA	2.0	1.6

4.4 Wind Direction

Figures 34, 35, and 36 show wind direction measurements for the WXT520 in May 2012. Here, there is a more consistent value with little diurnal variation, which is expected. We know that the wind pattern at the VLA site is that most of the time the wind comes directly from the West, following the direction of the trade winds at the latitude of the VLA. There is a similar phenomenon seen in daytime as with the other parameters (increased fluctuations), which we attribute to the same cause (convective heating is causing the surface layer to become turbulent, which results in higher fluctuations in instantaneous wind direction).

Figures 37 and 38 show differences between the measurement of the WXT520 (which we take as the most accurate of the measurements) and the DCS00 and LWA. For both of them, there is an obvious offset – about 40^{o} for the old VLA weather station, and about 15^{o} for the LWA weather station. In order to be sure that this is not due to a bias during quiet conditions (when all wind direction measurements become more uncertain), we created the histograms only using data when the wind speed as measured by the WXT520 was > 3 m/s (because by its technical specifications that is the cutoff where it becomes more accurate). Those are shown in Figures 39 and 40, both of which verify the characteristics of the histograms using all data. Table 4 shows the median offset of the distributions, as well as the standard deviation, if a single Gaussian is assumed. In the case of wind direction, we would be better served to use circular statistics (von Mises, with its concentration parameter) to estimate the properties of the distributions (e.g., Jammalamadaka & SenGupta 2001), but here the rough estimates provided by our simple analysis are sufficient.

We do not know how accurately the wind direction for the old VLA or LWA weather stations were set, but the fact that we expect the wind direction to average to 270^{o} over long periods, but we see a clear offset from that value in the raw WXT520 measurements of about 40^{o} makes us believe that the zero point for the old VLA weather station was set correctly, and the WXT520 was set about 40^{o} off where it should be. See above comments on the difficulty of setting this zero point. We made an adjustment in the software of the WXT520 in June 2012 to account for this offset. If a better technique for setting the zero point of the WXT520 is found, we must remember to take this offset out.

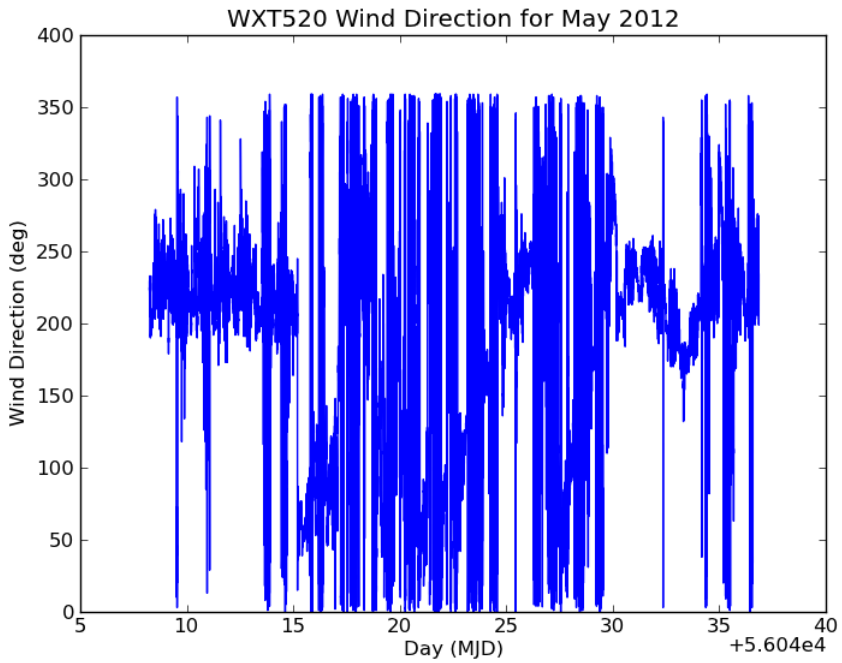

Figure 34. Measured wind direction for the month of May 2012 with the WXT520 instrument. Diurnal patterns are less pronounced than for the other weather parameters.

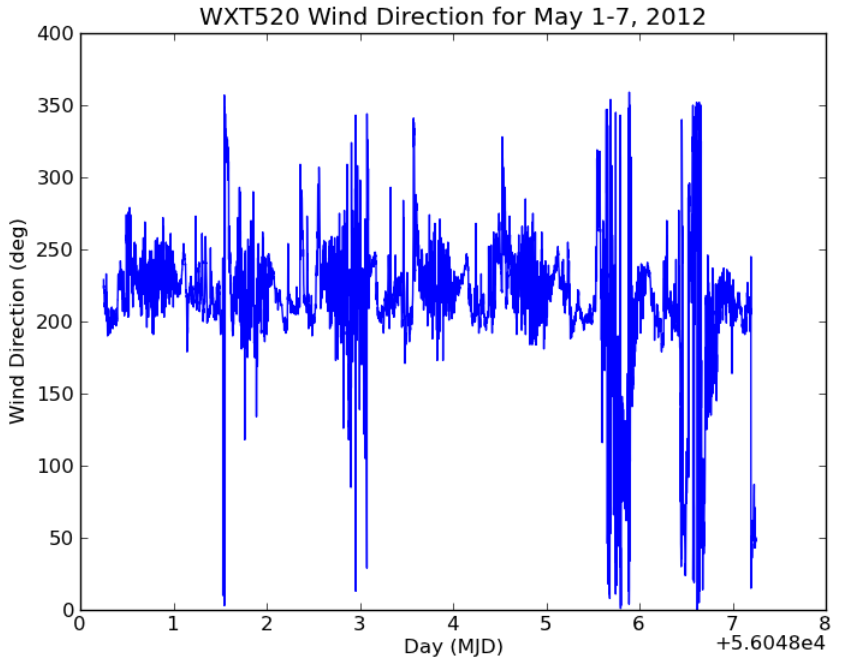

Figure 35. Measured wind direction for the week of May 1-7, 2012, with the WXT520 instrument. The fact that wind direction fluctuates more in daytime is apparent (the wind becomes more gusty). Note also the offset from the expected 270º.

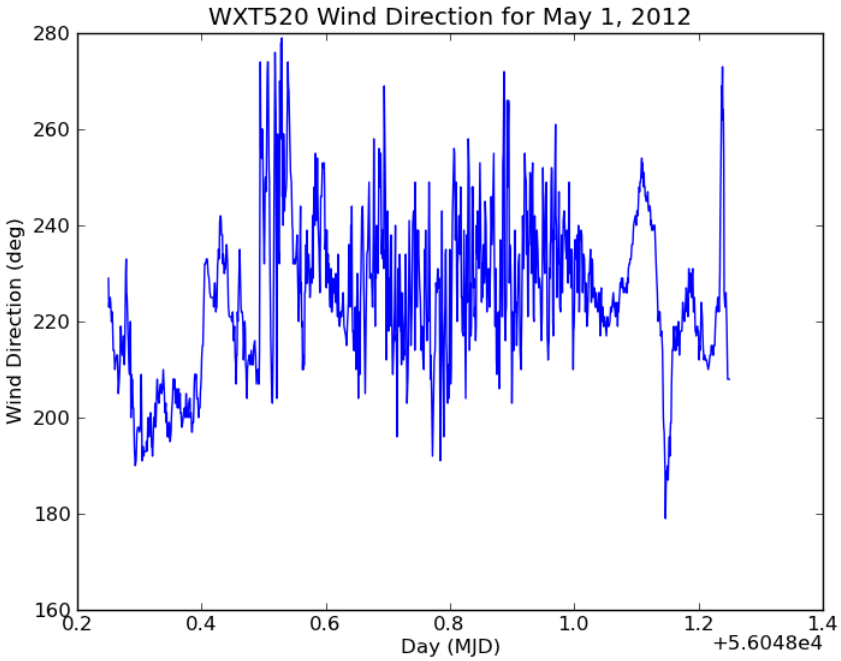

Figure 36. Measured wind direction for May 1, 2012, with the WXT520 instrument. The larger daytime fluctuations are now obvious.

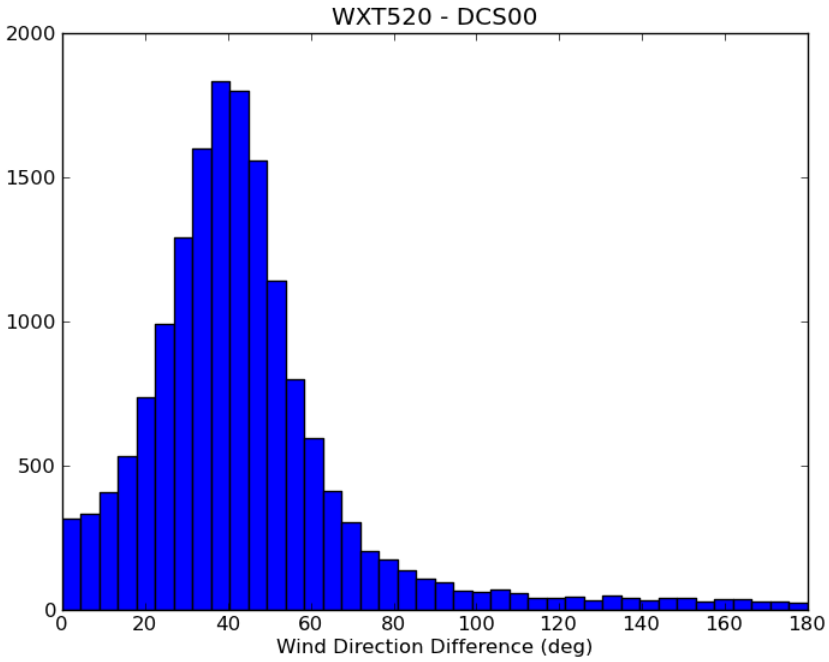

Figure 37. Histogram of the difference between the wind direction measurements of the WXT520 and the old VLA weather station for May 2012. An offset of about 40º is obvious.

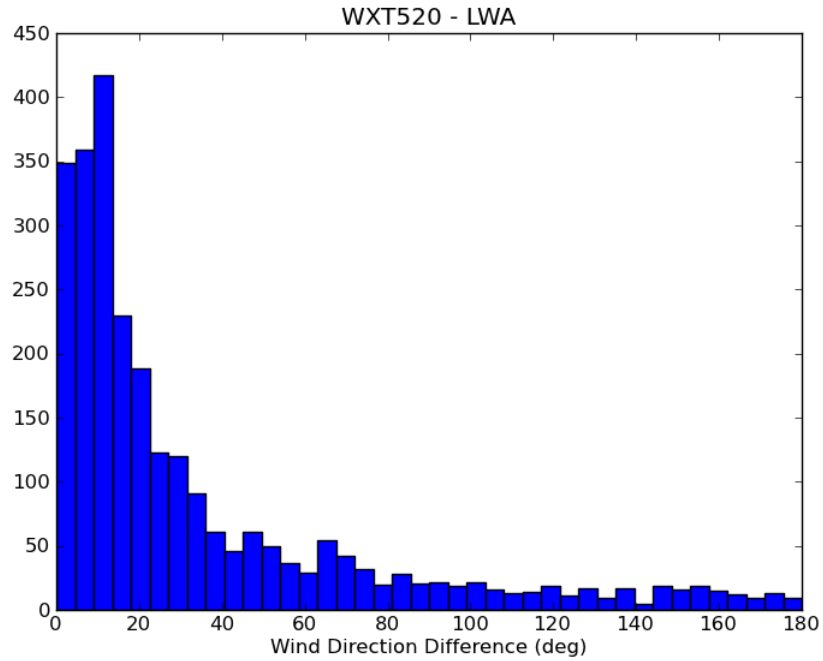

Figure 38. Histogram of the difference between the wind direction measurements of the WXT520 and the LWA weather station for May 2012. An offset of about 15° is obvious.

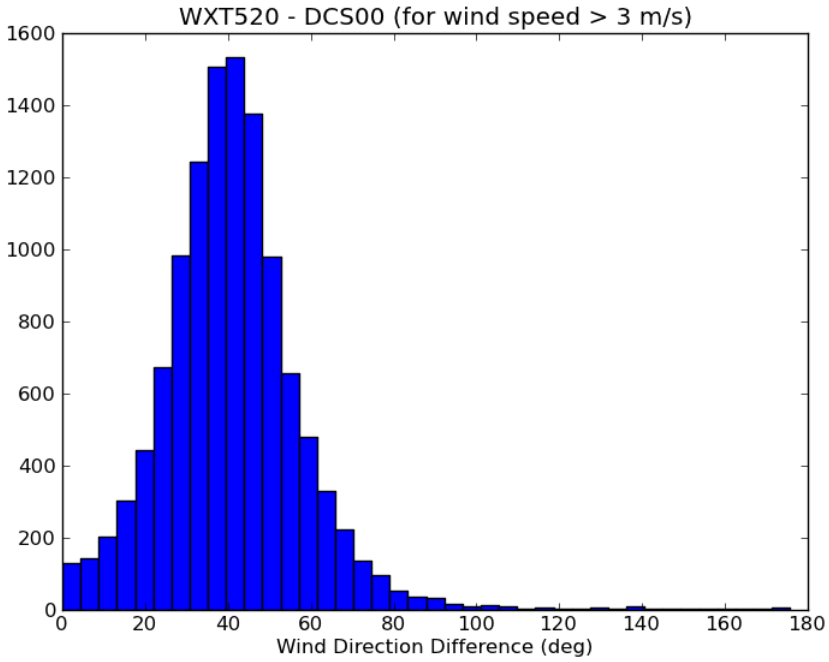

Figure 39. As Figure 37, but only for times when the wind speed measured by the WXT520 is > 3 m/s.

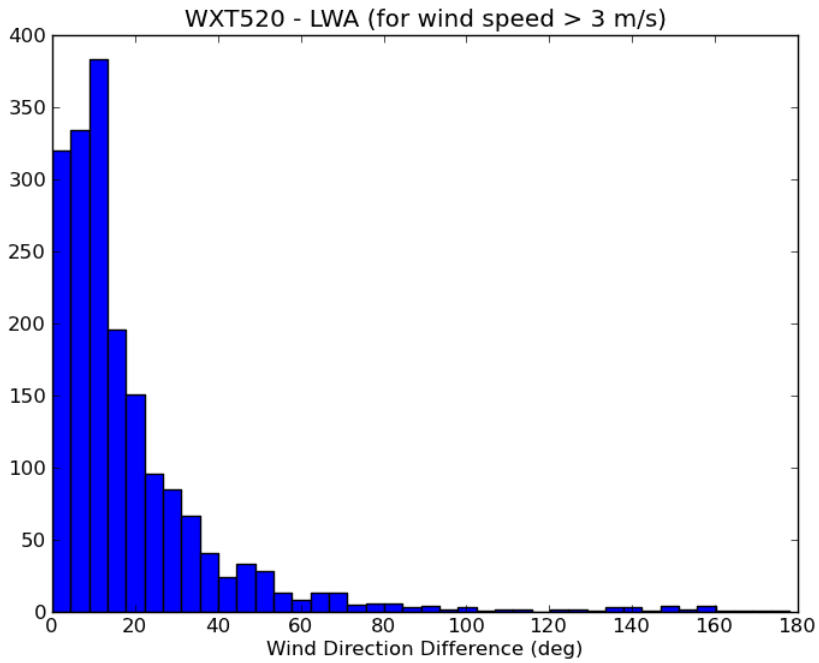

Figure 40. As figure 38, but only for times when the wind speed measured by the WXT520 is > 3 m/s.

Table 4. Median and standard deviation of differences in wind direction measurements for May 2012.

Quantity	Median (deg)	Std Dev (MAD * 1.4826) (deg)
WXT520 – DCS00	41	17
WXT520 – LWA	17	34
WXT520 – DCS00 (> 3 m/s)	40	14
WXT520 – LWA (> 3 m/s)	12	10

4.5 Pressure

Figures 41, 42, and 43 show pressure measurements for the WXT520 in May 2012. Here, there is again a diurnal variation, but more dominant is the variation on roughly one week timescales – i.e., changes due to local weather patterns. We see a slight indication that the pressure is more variable during daytime, but it is harder to tell because we are reaching the precision of the instrument (0.1 hPa), which you can easily see in Figure 43 as discrete levels.

Figures 44 and 45 show differences between the measurement of the WXT520 and the DCS00 and LWA. The offset with the old VLA weather station is small (about -2 mbar), as is the width of the distribution (about 3 mbar). The offset from LWA (-220 mbar) is clearly not valid, and we attribute this to a problem with the LWA pressure measurement. Table 5 shows the median offset of the distributions, as well as the standard deviation, if a single Gaussian is assumed.

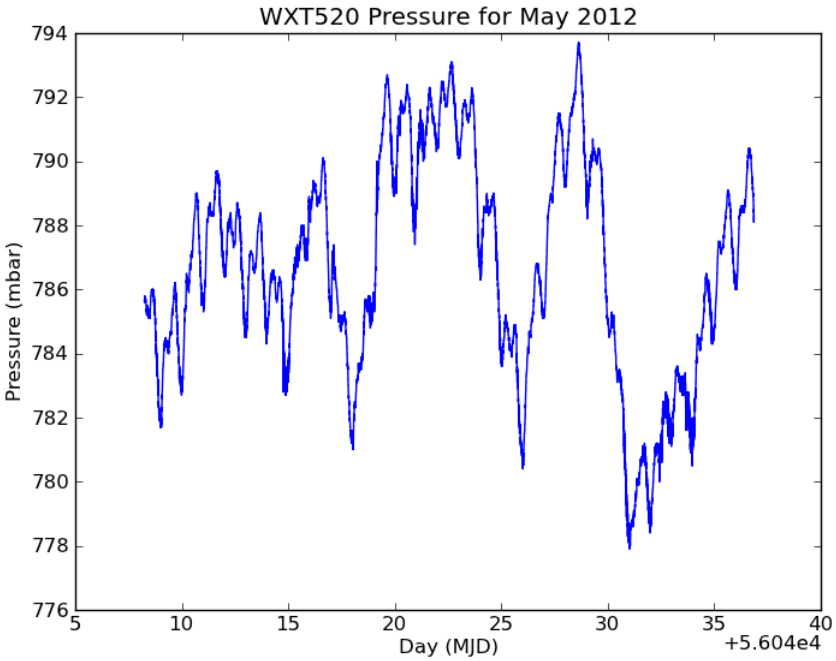

Figure 41. Measured pressure for the month of May 2012 with the WXT520 instrument. Diurnal variations can be seen, but they are dominated by local weather system passage (variations on roughly one week timescale).

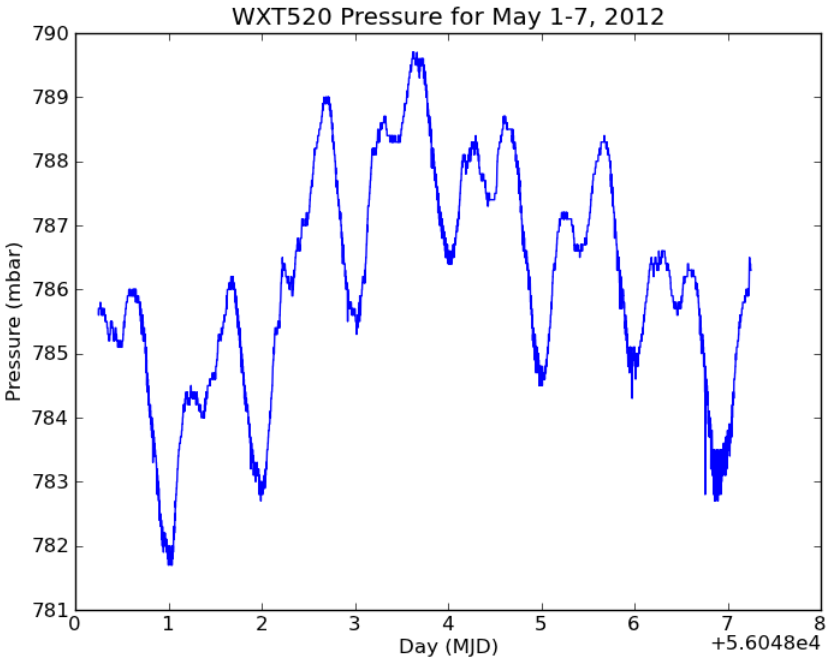

Figure 42. Measured pressure for the week of May 1-7, 2012, with the WXT520 instrument. Diurnal variations are now more obvious.

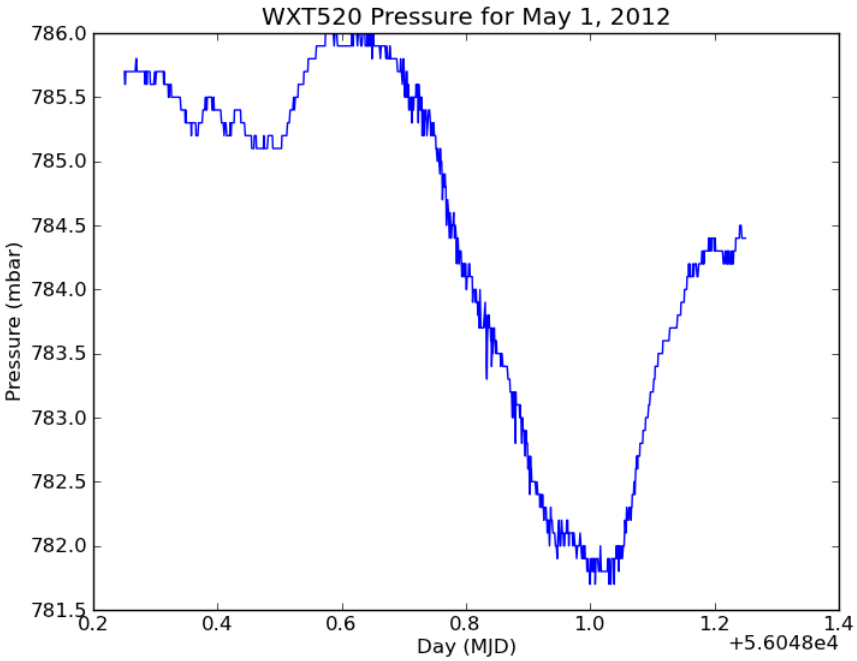

Figure 43. Measured pressure for May 1, 2012, with the WXT520 instrument. The diurnal variation is obvious, as is the fact that we have reached the precision limit of the device.

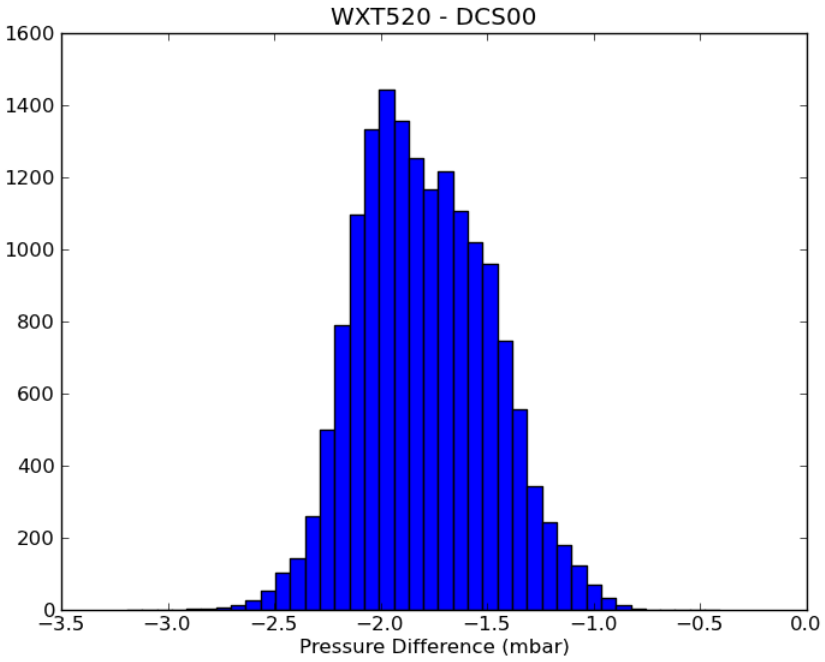

Figure 44. Histogram of the difference between the pressure measurements of the WXT520 and the old VLA weather station for May 2012. The offset and width of the differences are both small.

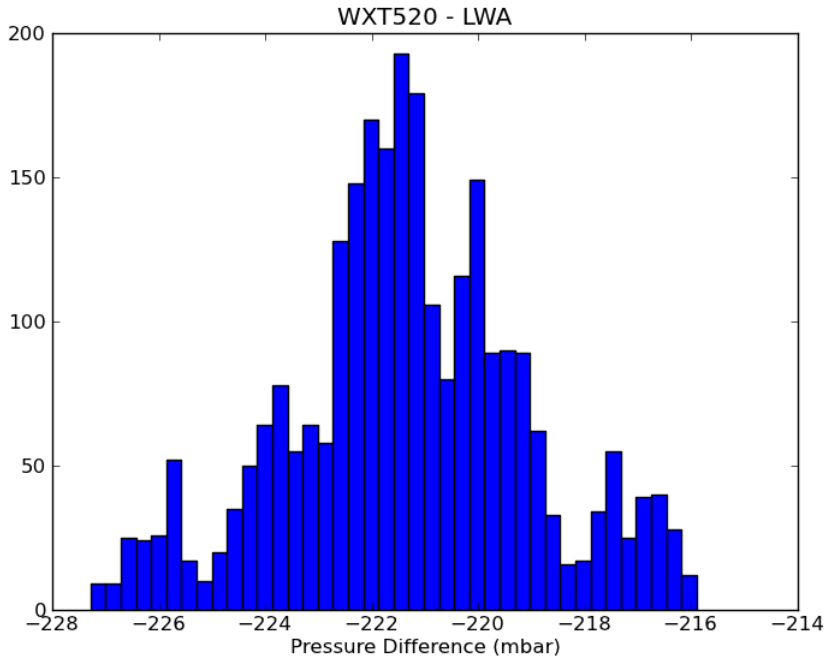

Figure 45. Histogram of the difference between the pressure measurements of the WXT520 and the LWA weather station for May 2012. The offset is huge, and cannot be real – we suspect an error in the LWA measurement.

Table 5. Median and standard deviation of differences in pressure measurements for May 2012.

Quantity	Median (mbar)	Std Dev (MAD * 1.4826) (mbar)
WXT520 – DCS00	-1.8	0.3
WXT520 – LWA	-220	2.0

5.0 Interface

The weather station instrumentation is accessed via the M352 MIB. The values and alerts from this MIB are multicast on the internal network as well as being written to the monitor database archive. Because of this, there is no reason for the casual user to need direct access to the instrumentation via the MIB; desired quantities should be retrieved either from the archive (for internal users) or the wunderground website (see below – for external users). External users can also use the helpdesk to request quantities not stored at wunderground.

6.0 Display

For internal users, the Array Operators Interface has a very nice weather display screen. It shows current weather conditions and history of selected quantities – API/Wind, Temp/Press, Radar, SkyCam, Rain, or Pyranometers. Figure

46 shows screenshots of these various displays (except the sky camera, which is not installed yet, and the rain – we haven't had rain in a long time!).

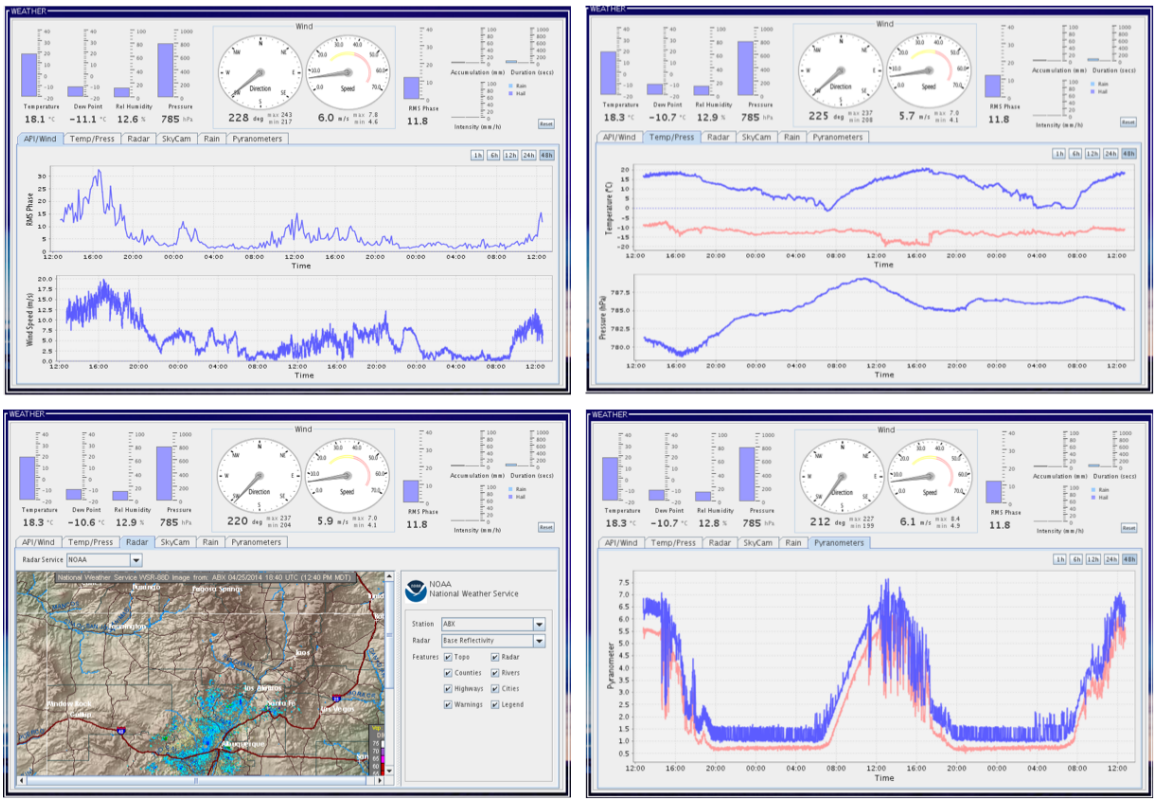

Figure 46. Tabs within the AOI weather screen. Upper left is the 'API/Wind' tab, which shows API saturation phase, and wind speed. Upper right is the 'Temp/Press' tab, which shows temperature and pressure. Lower left is the 'Radar' tab, which shows the current local radar. Lower right is the 'Pyranometers' tab, which shows the pyranometers. For the locally measured quantities, the past 48 hours are shown.

7.0 Wunderground

We transmit values of temperature and relative humidity as measured by the HMT337, and pressure and wind speed, direction, and gust as measured by the WXT520, to wunderground.com every five minutes. We do this to provide an easily accessible web-based site from which anybody can see what the weather at the VLA is like currently (or in the past). The direct web URL for the VLA weather station is: http://www.wunderground.com/personal-weather-station/dashboard?ID=KNMSOCOR8.

8.0 Conclusions

The new weather station at the VLA is a big improvement over the old one. It is on a higher (and more sturdy) tower (though, admittedly, the lack of ability to lower the tower has made some maintenance more difficult). It has a more robust suite of instrumentation than the old weather station, with duplication of measured

quantities. The instruments are calibrated with NIST traceability. And we have much better display software for the quantities measured by it.

References

Butler, B. & R. Perley, 2008. Accuracy Requirements for EVLA Meteorological Measurements, EVLA Memo 126.

Clark, B., 1987. Precision of Meteorological Measurements, VLA Scientific Memo 157.

Hampel, F. R., 1974. The Influence Curve and its Role in Robust Estimation, Journal of the American Statistical Association, 69, 383-393.

Jammalamadaka, S. R., & A. SenGupta, Topics in Circular Statistics, World Scientific, 2001.

Ranta-aho, T. & L. Stormbom, 2002. Real Time Humidity Measurement Using the Warmed Sensor Head Method, 4th Int. Symp. On Humidity and Moisture ISHM 2002, Taipei, pp. 583-588.